Atmos. Chem. Phys., 7, 4257–4266, 2007
www.atmos-chem-phys.net/7/4257/2007/

Atmospheric Chemistry and Physics

A case study on biomass burning aerosols: effects on aerosol optical properties and surface radiation levels

A. Arola[1], **A. Lindfors**[2], **A. Natunen**[1,3], **and K. E. J. Lehtinen**[1]

[1]Finnish Meteorological Institute, Kuopio, Finland
[2]Finnish Meteorological Institute, Helsinki, Finland
[3]Tampere University of Technology, Tampere, Finland

Received: 5 April 2007 – Published in Atmos. Chem. Phys. Discuss.: 16 May 2007
Revised: 8 August 2007 – Accepted: 16 August 2007 – Published: 20 August 2007

Abstract. In spring 2006, biomass burning aerosols from eastern Europe were transported extensively to Finland, and to other parts of northern Europe. They were observed as far as in the European Arctic. In the first part of this paper, temporal and spatial evolution and transport of these biomass burning aerosols are monitored with MODIS retrieved aerosol optical depth (AOD) imagery at visible wavelengths (0.55 μm). Comparison of MODIS and AERONET AOD is conducted at Tõravere, Estonia. Then trajectory analyses, as well as MODIS Fire Mapper products are used to better understand the type and origin of the air masses. During the studied four-week period AOD values ranged from near zero up to 1.2 at 0.55 μm and the linear correlation between MODIS and AERONET was very high ($\sim$0.97). Temporal variability observed within this four-week period was also rather well explained by the trajectory analysis in conjunction with the fire detections produced by the MODIS Rapid Response System. In the second part of our study, the surface measurements of global and UV radiation at Jokioinen, Finland are used to study the effect of this haze episode on the levels of surface radiation. We found reductions up to 35% in noon-time surface UV irradiance (at 340 nm) as compared to typical aerosol conditions. For global (total solar) radiation, the reduction was always smaller, in line with the expected wavelength dependence of the aerosol effect.

1 Introduction

The atmosphere in southern Finland is generally relatively clean from aerosols, particularly in non-urban areas. However, haze episodes, that vary in strength, take place occasionally. They are observed particularly in spring, but sometimes also in autumn, due to long-range transported aerosols. The episode observed in spring 2006 was exceptionally severe, when biomass burning aerosols from eastern Europe were transported extensively to Finland, and to other parts of northern Europe. In April and May 2006, a large number of widespread fires occurred in the Baltic countries, western Russia, Belarus and Ukraine. They were initiated and spread by the smaller fires owing to the practice of farmers to burn agricultural fields ahead of the growing season in order to make them more fertile.

Stohl et al. (2007) presented a detailed analysis of this episode using various measurements of air pollution in the European Arctic. Our paper concentrates on the effects of this episode on aerosol optical properties and surface radiation levels in southern Finland and its near surroundings. First, we study the spatial and temporal evolution of particulate matter spread from these forest fires. For this, we used trajectory analysis and MODIS satellite-retrieved aerosol optical depth (AOD). In addition, the MODIS Fire Mapper product was used for achieving a better understanding of the variability of the fires in the source region of this plume of biomass burning aerosols. Finally, to ensure that the MODIS AOD data are quantitatively correct, they were compared with ground-based measurements at the AERONET (AErosol RObotic NETwork) station of Tõravere, Estonia.

In the second part of this paper, we use this analysis of the prevailing aerosol conditions for investigating the effects of this episode of biomass burning aerosols on surface radiation levels at Jokioinen, southern Finland. Already a visual examination of ultraviolet (UV) irradiance measurements at Jokioinen during this episode revealed significant reductions compared to what would be expected under typical aerosol conditions in southern Finland this time of the year. Thus, it was clear from the start that these biomass burning aerosols exerted a strong effect on the amount of UV radiation reaching the surface. Earlier results indeed indicate that aerosols can cause a considerable reduction in the

Correspondence to: A. Arola
(antti.arola@fmi.fi)

surface UV irradiance. In the extreme, this reduction can be up to 50% (e.g., Reuder and Schwander, 1999; Krotkov et al., 1998), although more typical values for this reduction associated with biomass burning aerosols range from 15–35% (e.g., Latha et al., 2004; Kalashnikova et al., 2007). The net effect that atmospheric aerosols exert on the surface radiation is a complex matter and strongly depends on both scattering and absorption characteristics, which in turn depend on wavelength and relative humidity. Therefore, different commonly observed tropospheric aerosol types (e.g. sulfate, dust, organic carbon, black carbon, and sea salt) impose different radiative effects, mainly due to the differences they have in the absorption efficiency. For instance, Balis et al. (2004) showed that for the same AOD, the UV-B irradiances at the Earth's surface can show differences up to 10%, which can be attributed to differences in the aerosol type. Our study focuses on the effect induced by a strong event of biomass burning particles embedded in the continental background aerosols.

As the transmission of the atmosphere containing aerosols typically increases with increasing wavelength, the aerosol-induced reduction is expected to be more pronounced at shorter wavelengths (e.g., Erlick and Frederick, 1998; Kalashnikova et al., 2007). By combining surface irradiance measurements at Jokioinen and radiative transfer modeling with information on the aerosol conditions, we investigated the effect of this spring time haze episode on surface radiation levels. Our analysis includes measurements of both UV and global radiation (total solar), and thus also highlights the wavelength dependence of the aerosol effect.

2 Data and methods

2.1 MODIS

There are currently two MODIS (MODerate Resolution Imaging Spectroradiometer) instruments, the first launched on 18 December 1999 onboard the Terra and the second on 4 May 2002 onboard the Aqua platform (Remer et al., 2005). MODIS aerosol products are freely available and are extensively used, for instance for studies of aerosol direct and indirect radiative effects (e.g., Christopher and Zhang, 2004; Yu et al., 2004). The MODIS AOD data are available over the oceans globally and over a portion of the continents. Further, the aerosol size distribution is derived over the oceans, and the aerosol type over the land surface. We used Level 2 data from Collection 4, at the spatial resolution of 10 by 10 km, and extracted the parameter within 0.2 degree in latitude and longitude from the given location. We used the data from both Terra and Aqua platforms.

In addition to AOD, we used also the Ångström exponent, available from MODIS aerosol products and estimated from AOD values at 0.66 μm and 0.47 μm. The wavelength dependence of AOD is usually described by the following formula called Ångström law:

$$\mathrm{AOD}_\lambda = \beta \cdot \lambda^{-\alpha}, \quad (1)$$

where λ is in μm. Ångström α and β parameters are also often called Ångström exponent and turbidity parameter, respectively. We used the MODIS Ångström exponents to relate the MODIS AOD at 0.55 μm to ultraviolet wavelengths (0.34 μm). Admittedly, some uncertainty is introduced when estimating AOD at UV wavelengths using Ångström α retrieved in the visible band.

2.2 AERONET

AERONET (AErosol RObotic NETwork)is a world-wide network of automated ground-based CIMEL sunphotometers providing spectral aerosol optical depth (AOD), inversion products of other aerosol optical properties, such as single scattering albedo (SSA) and the column integrated aerosol size distributions above the measurement site (Holben et al., 1998).

There are some differences in the wavelengths that are measured depending on the exact type of CIMEL. Typically the sunphotometers, that are currently installed, take measurements of the direct sun radiance at eight spectral channels (340, 380, 440, 500, 670, 870, 940 and 1020 nm) with triplet observations per wavelength and diffuse sky radiances at four spectral channels (440, 670, 870 and 1020 nm).

For our study, we used the version 1.5 data of Tõravere (58.26 N, 26.46 E), as obtained through the AERONET web-service. In addition to AOD that is a measure of aerosol total extinction (scattering and absorption), we also used SSA to constrain our radiative transfer simulations. SSA is the ratio of scattering to total extinction. Thus a value of one means that only scattering takes place and the smaller the value of SSA, the larger is the contribution from absorption.

2.3 Surface observations at Jokioinen

The observatory of Jokioinen (60.81 N, 23.50 E) is located in a rural area in southern Finland, surrounded by crop fields and mixed boreal forest. The spectral surface UV irradiance at Jokioinen is measured with a Brewer MKIII double monochromator spectrophotometer. The instrument is calibrated regularly and the data is corrected for major instrumental errors. The Brewer at Jokioinen meets the WMO level S-2 requirements (Seckmeyer et al., 2001) for detection of trends. More detailed information on the measurement procedure is given in Koskela et al. (1994).

In this study, the UV irradiance at 340 nm was chosen for closer examination, since it is not influenced by ozone absorption to any great extent. In addition, we used ancillary data including global radiation (300–3000 nm) measured with a Kipp and Zonen CM11 pyranometer, sunshine duration measured with an electronic sunshine recorder (Lindfors et al., 2003) and SYNOP cloud amount.

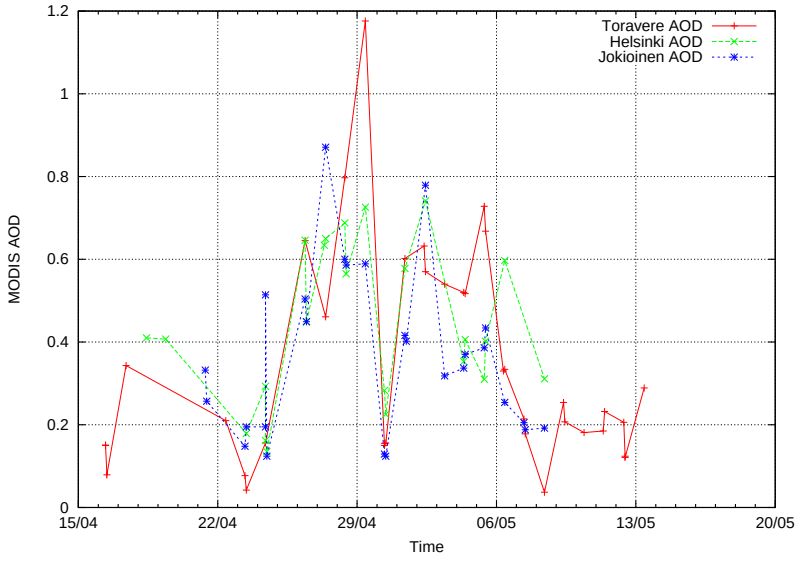

Fig. 1. AOD values at 0.55 μm from MODIS for Tõravere, Estonia and Helsinki and Jokioinen, Finland.

3 Results

Figure 1 shows MODIS derived AOD values at 0.55 μm during a four-week-period for Tõravere as well as for Helsinki and Jokioinen in Finland. It is apparent that there is a strong temporal variability in AOD during this biomass burning episode, with the highest values reaching as high as 1.2. In the following, we first investigate the temporal variability in more detail and compare AERONET and MODIS AOD data. Thereafter, we examine the effect of this plume of biomass burning aerosol on the surface irradiances of both UV and global radiation at Jokioinen.

3.1 Comparison of MODIS and AERONET derived AOD

In the comparison of AERONET and MODIS AOD at Tõravere, we required that the time difference between MODIS overpass and the ground-based AOD measurement was less than one hour. As a spatial comparability requirement, we included MODIS AOD data only if the distance from the center of MODIS pixel to the station was less than 0.2 degree, both in latitude and longitude.

Figure 2 shows the comparison between MODIS and AERONET measurements at 0.55 μm. The data period covered is from 17 April to 11 May 2006. The correspondence is very good with a linear correlation coefficient of $\sim$0.97. There are almost 30 observations that meet the spatial and temporal selection criteria. The label "mean" in the figure refers to the absolute difference, that is calculated by taking the difference of MODIS and AERONET AOD. The standard deviation is calculated from these differences.

Figure 3 shows the same comparison as in Fig. 2, but this time as time series. Interestingly, there are few days when drastically cleaner air mass is transported into the region and AOD is temporarily decreased, most distinctly on 30 April.

The observed good correlation is likely partly due to the fact that this period exhibited a clear range of AOD values; it included both very high AOD values but also significantly lower values during some days, when the air masses arrived from outside biomass burning areas. Both MODIS and AERONET show, for instance, the strong decline in AOD on 30 April. These cases are discussed in more detail below.

We want to emphasize that the period in our study is rather short to make any comprehensive comparison against previous validation studies. Moreover, since the earliest validation studies (e.g., Chu et al., 2002; Remer et al., 2002) the MODIS aerosol algorithm has been further modified and improved. However, generally our results seem to be in agreement with, for instance, Remer et al. (2005) who compared MODIS AOD against a great number of AERONET stations. They found slight overestimation at low optical thicknesses, while the opposite happened at the highest aerosol loadings. They speculated that the surface reflectance treatment in the satellite retrieval would be the likely reason for the overestimation, while the insufficient light absorption is causing the overestimation at high AOD. Currently, the Collection 5 version of MODIS AOD are already available, and these data are likely improved in these respects.

In order to study this variability in AOD in more detail, we used HYSPLIT- based trajectories (Rolph, 2003) to determine the origin of air masses arriving at Tõravere, as well as MODIS Fire Mapper products to give an idea about the location and extent of fires at each day. Figure 4 shows the active fires detected by the MODIS Rapid Response System from 28 April to 30 April. According to these data, it seems

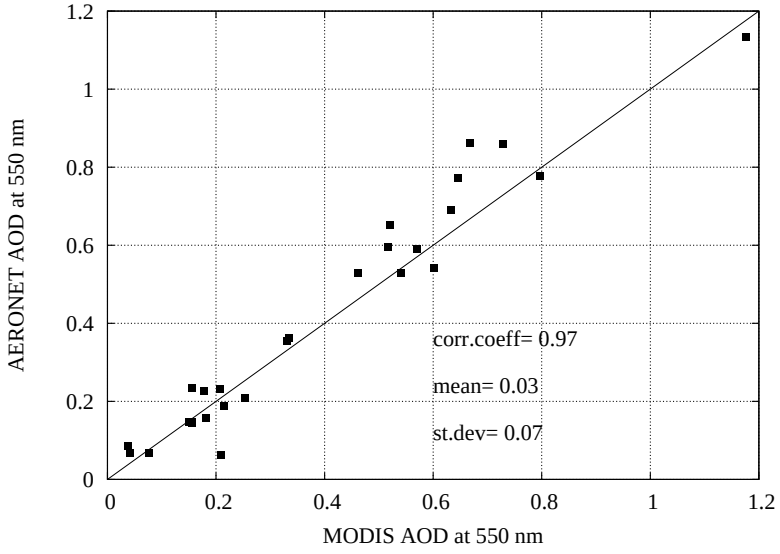

Fig. 2. Scatter plot of MODIS and AERONET AOD at 0.55 μm for Tõravere. The mean and standard deviation are calculated from the difference of MODIS and AERONET AOD.

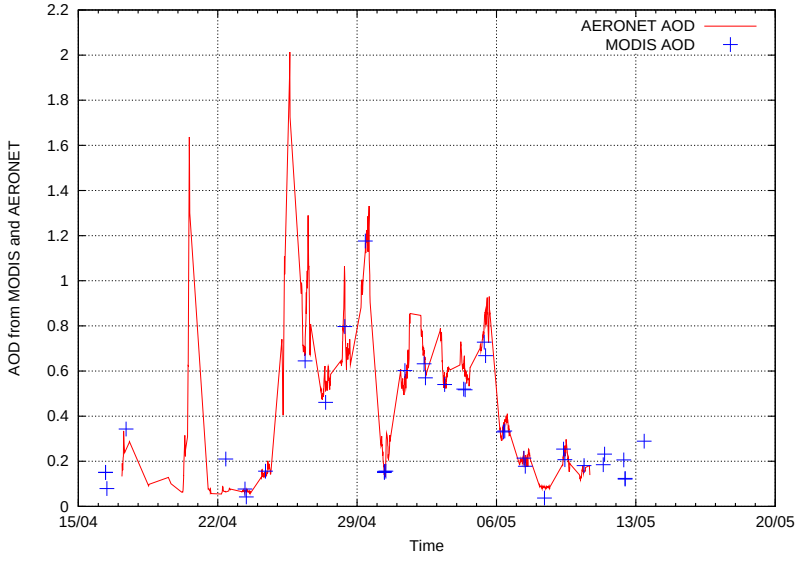

Fig. 3. Time series of comparison between MODIS and AERONET AOD at 0.55 μm for Tõravere.

that there was a slight decrease in the number of active fires on 29 April, one day before the low AOD was measured at Tõravere, at a distance from these fire areas.

If the slightly ceased fires on 29 April are combined with the trajectory analysis, one finds further support for the very low AOD on 30 April. In Fig. 5 a set of trajectories are shown that arrived at different altitudes at Tõravere, 12:00 UTC on 30 April. The trajectories one day before, as well as one day after (not shown), indicate that the air masses arrived dominantly from the south-east, from the region of active biomass burning, while the weather system on 30 April brought temporarily more easterly and thus cleaner air.

The temporal short-term variability measured by the ground-based instrument is also supported by the spatial variability, the large-scale view that the space-borne instrument is able to capture. Shown in Fig. 6 is the MODIS AOD at 1 by 1 degree resolution clearly illustrating how the tongue of cleaner air is pushing for large areas in Estonia and Finland on 30 April supporting our results.

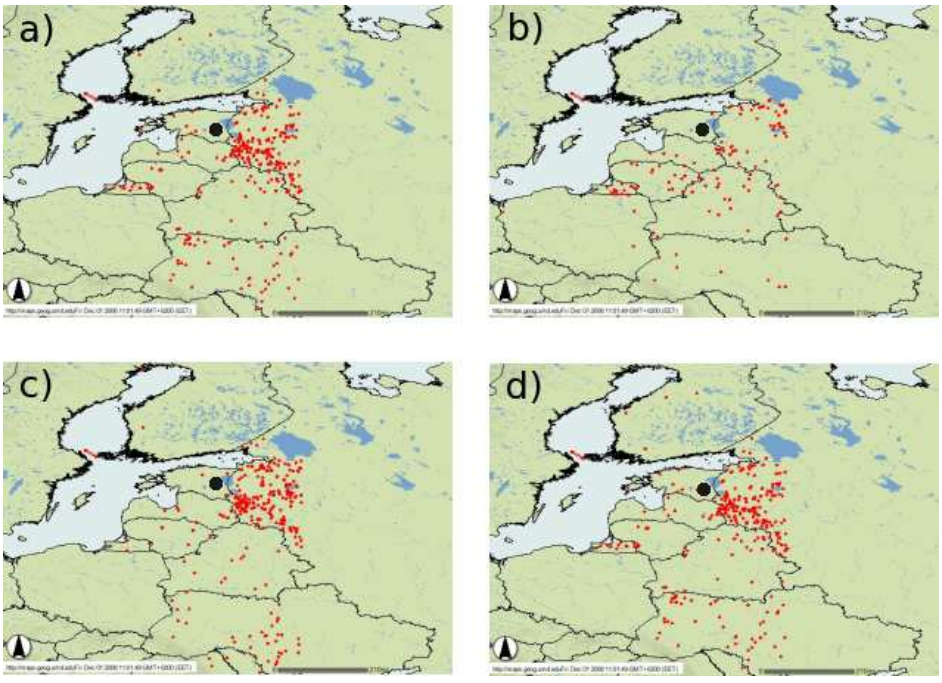

Fig. 4. MODIS Firemapper detection for the following days **(a)** 28 April, **(b)** 29 April, **(c)** 30 April, **(d)** 1 May. Tõravere is indicated by a black dot.

3.2 Aerosol effect on solar UV and global radiation

As aerosols vary not only in space and time, but also in shape and composition, so does the effect they exert on radiation; ultimately, this effect is determined by the radiative properties of the individual aerosol particles together with how they are distributed within the atmosphere. Usually, however, such detailed information is not available. Instead, various approximations may be used, for instance, standard aerosol properties for different source regions or aerosol climatologies (Shettle, 1989; Koepke et al., 1997). On the other hand, if measurements on the aerosol properties are available, more detailed information can be added to these standard cases.

Our approach for investigating the effect of biomass burning aerosols on the surface irradiances of both UV and global radiation was to use radiative transfer modeling by the libRadtran package (Mayer and Kylling , 2005). The radiative transfer simulations were performed as follows: we assumed the standard atmospheric profiles for mid-latitude summer by Anderson et al. (1986), a surface albedo of 0.05 for UV wavelengths and 0.12 for global radiation, and we used the disort2 solver of the radiative transfer equation with 8 streams. For calculations of global radiation, we used the kato2 parameterization (Kato et al., 1999) included in libRadtran, and a constant total water vapor column of 13 kg/m^2 representative for spring in southern Finland (according to the ERA-40 reanalysis; Uppala et al., 2005). When simulating the UV irradiances, the slit function of the Brewer at Jokioinen was taken into account, and the calculations were performed using a constant total ozone column of 380 DU.

Figure 7 shows the weather conditions at Jokioinen during this haze event. The global radiation and sunshine duration both indicate that the weather in general was sunny during this period. This was furthermore supported by the cloud observations (not shown).Thus, all radiative transfer simulations were performed assuming cloudless skies, which excludes one significant source of uncertainty, namely clouds, and thus makes the analysis of the data easier. The following days were virtually cloud free and hence chosen for closer examination: 24, 26, 27, and 30 April, as well as 1 and 5 May. Unfortunately, no Brewer UV measurements were available for 5 May, which was hence left out of our analysis.

Regarding the aerosol setup of the model, we defined two different cases: (i) a clean model run with background aerosols resembling the typical conditions this time of year at Jokioinen, and (ii) a polluted run with realistic aerosols, as observed during this episode. For both cases, we assumed the rural background aerosol profile, as defined by Shettle (1989). These settings were then successively adjusted as follows. First, the aerosol optical depth and its wavelength dependence were scaled according to the Ångström law (Eq. 1). Thereafter, the single scattering albedo was defined. In the polluted model run, the Ångström parameters (α and β) were taken from the MODIS measurements, while for the clean run, they were set to 1.4 and 0.04, respectively,

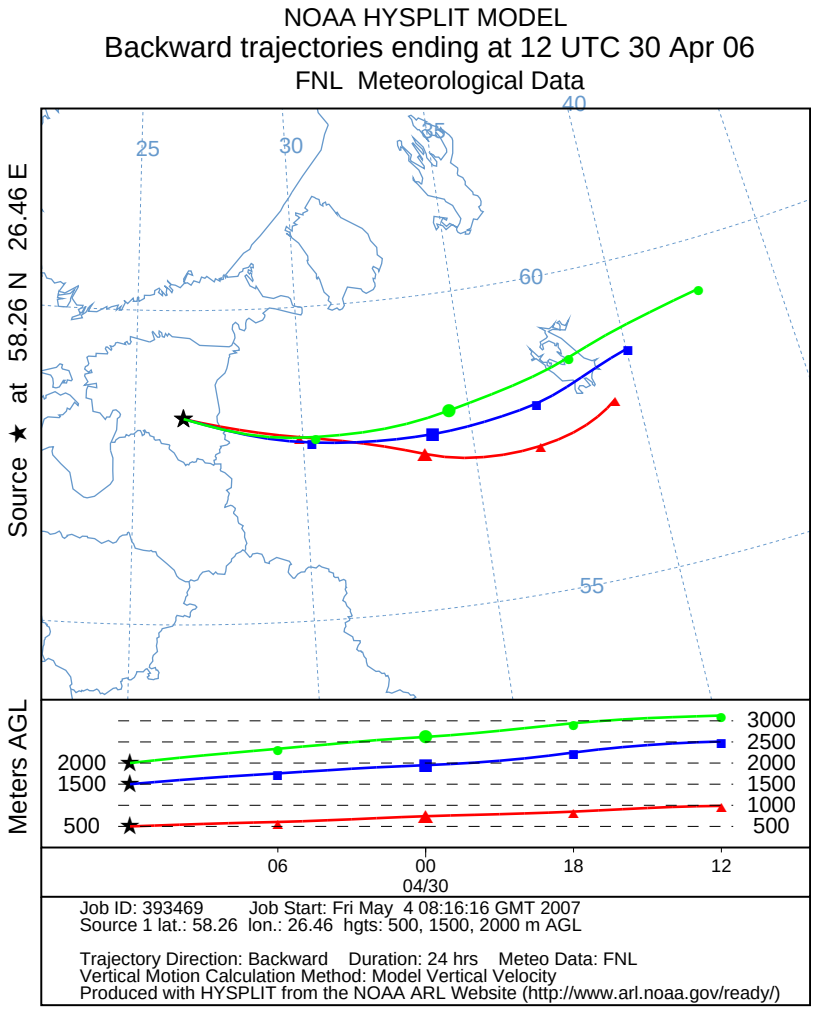

Fig. 5. Trajectories that arrive in Tõravere (shown by a star) at different altitudes, 30 April.

corresponding to an AOD of 0.18 at 340 nm and 0.09 at 550 nm. Since no estimates of the single scattering albedo were available for Jokioinen during this episode, we set its value to 0.92 in the polluted run. This corresponds to the mean value during the period of interest as measured by the AERONET station at Tõravere. For the clean run, the single scattering albedo was set to 0.96 in agreement with the rural background aerosol type.

The impact of aerosols on surface radiation depends not only on the aerosol loading and absorption efficiency, but also on the the solar zenith angle which modifies the optical path through the atmosphere. Because our analysis was based on MODIS AOD data available for times near local noon, we focused on the aerosol-induced decrease in the noon irradiances. As mentioned above, our analysis included days from 24 April to 1 May (Fig. 8) corresponding to noon solar zenith angles between 48 and 45.7.

Figure 8 shows the results of our radiative transfer calculations in comparison with measurements. It is clear that the polluted run agrees much better, and rather satisfactorily, with the measurements of both UV and global irradiances. The discrepancies between modeled and measured noon irradiances range from –3% (on 26 April) to +1% (27 April) for both UV and global radiation. The effect of aerosols on the surface irradiances is seen as the difference between the clean background simulation and the measurements. During most days, there was a clear reduction in the surface irradiances because of the prevailing aerosol conditions. Two cleaner days constitute the exception here: 24 April, before the onset of the aerosol episode, and 30 April, a clean day in the middle of the episode (as discussed above). Especially for 24 April, the agreement between the clean model run and the measurements give confidence in that the clean run indeed represents the typical aerosol conditions at Jokioinen this time of the year. As expected based on the typical wavelength dependence of the aerosol effect, the aerosol-induced reduction is more pronounced in the UV than for global radiation. In the UV, a reduction of roughly 35% (25%) is seen

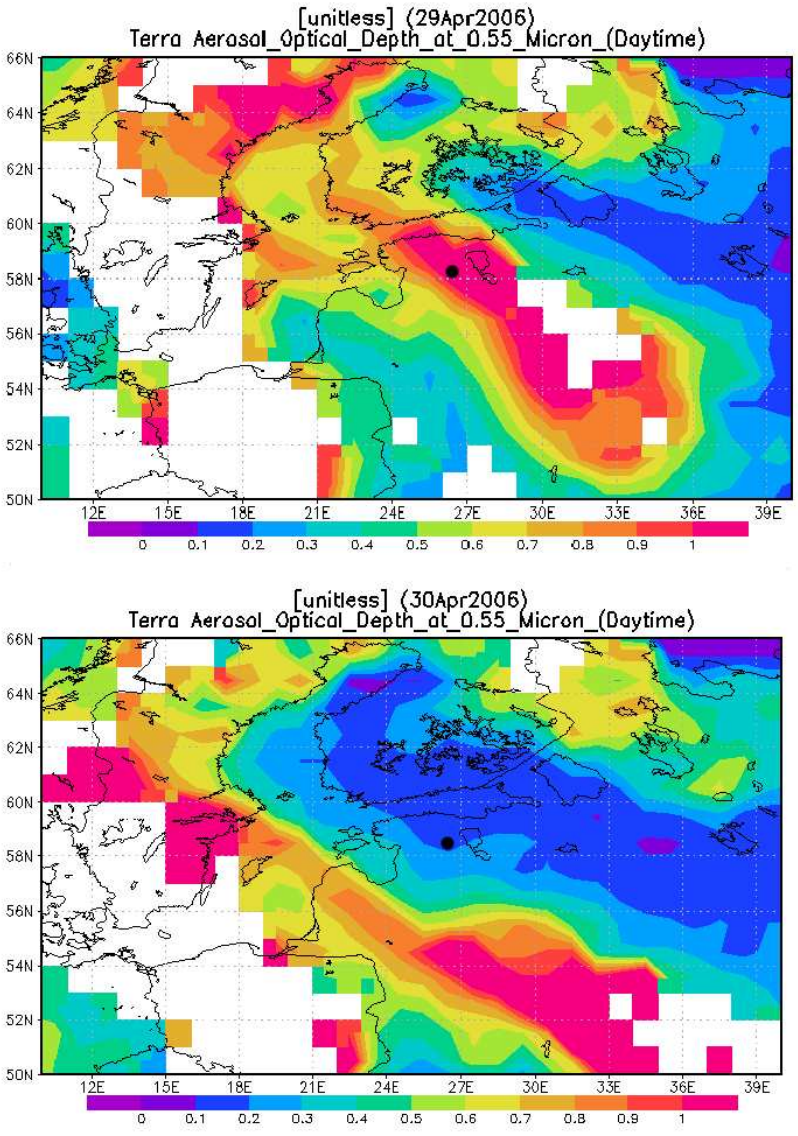

Fig. 6. AOD values for the Baltic region on 29 and 30 April. Tõravere is indicated by a black dot.

on 27 April (26 April). This is the same order of magnitude as found by, for instance, Kylling et al. (1998) for summer conditions in Greece. Recently, Kalashnikova et al. (2007) studied the influence of biomass burning aerosols on the UV irradiance in Australia. Also they found reductions of similar magnitude. In the present work, we found significant reductions (15% on 27 April) also in the global irradiances. It is emphasized that both Kylling et al. (1998) and Kalashnikova et al. (2007) investigated the aerosol effect on surface irradiance with respect to aerosol-free conditions, while we included typical aerosol conditions in our clean run, as described above. Therefore, in our case, a comparison against aerosol-free conditions would have resulted in few percent higher reduction in UV.

4 Conclusions

The atmosphere in southern Finland is generally relatively clean from aerosols, particularly in non-urban areas. However, haze episodes in spring and autumn occur occasionally and the event in spring 2006 was exceptionally strong. During that time, biomass burning aerosols from eastern Europe were transported extensively to Finland, and to other parts of northern Europe. Our paper describes a compact study, exploiting surface irradiance levels measured at Jokioinen, Finland and aerosol optical depth (AOD) measurements at Tõravere, Estonia during this same episode. Moreover, MODIS AOD measurements were obtained for these sites and MODIS imagery was also used for monitoring of spatial

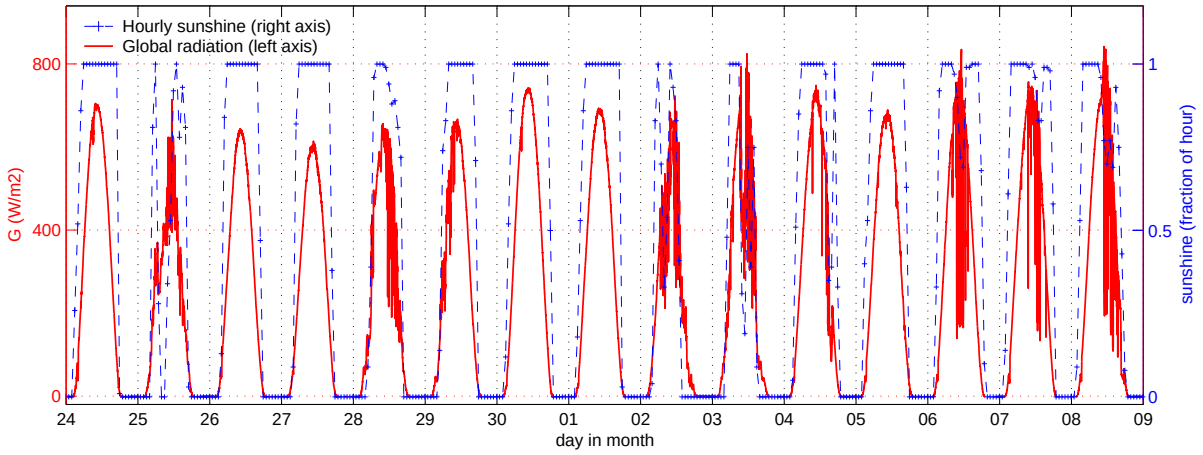

Fig. 7. Global radiation and hourly sunshine duration for the period 24 April to 8 May 2006. The global radiation data is minute-wise, which means that even short disturbances by clouds in the radiation data are detected.

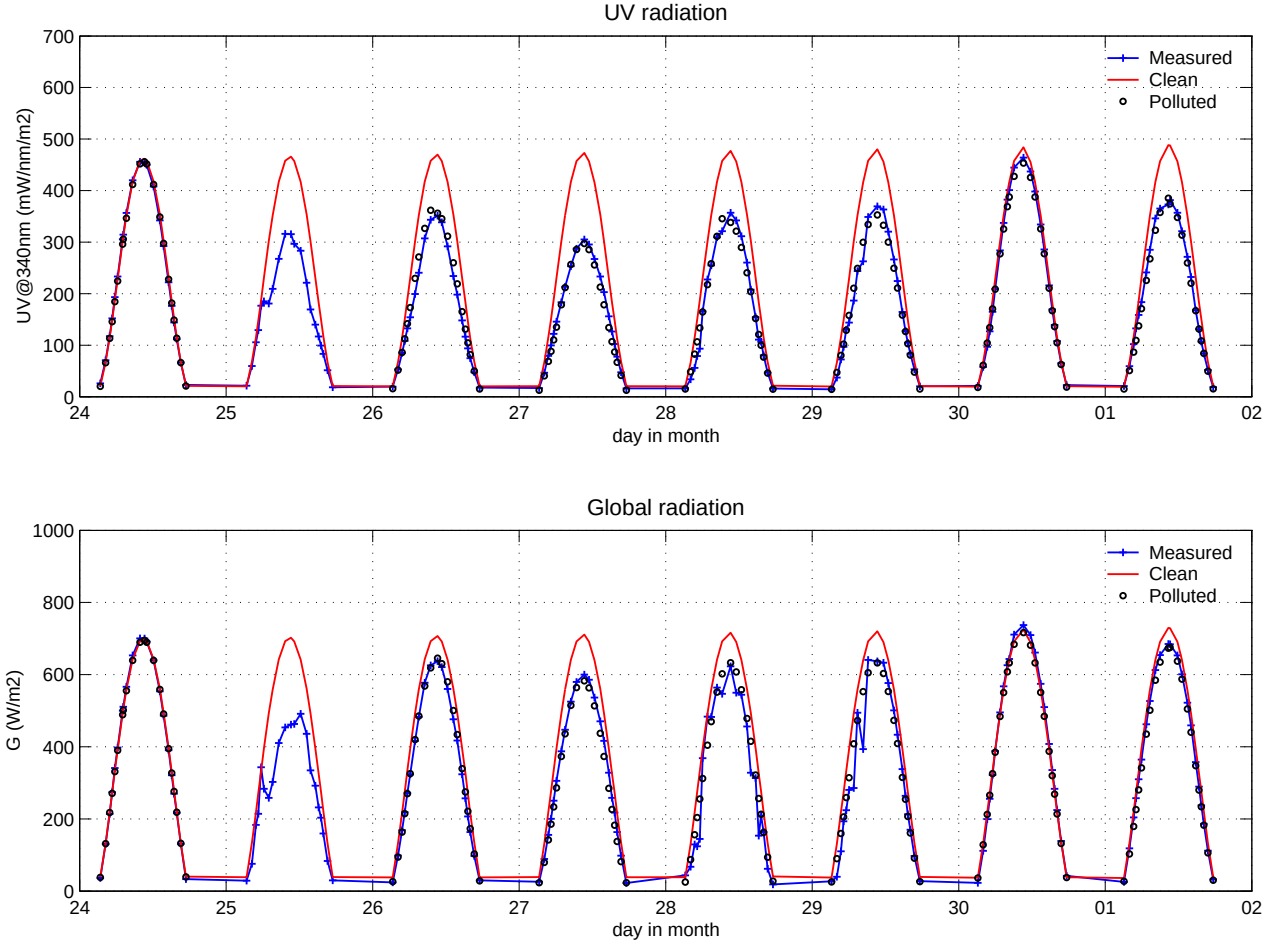

Fig. 8. Measured irradiances (blue) together with irradiances simulated using different aerosol settings (red – clean model run; black – polluted model run): (upper panel) UV irradiances at 340 nm, (lower panel) global irradiances. MODIS data for 25 April were not available.

and temporal evolution of particulate matter spread from these fires.

In the first part of our study, we compared AERONET and MODIS AOD at Tõravere, Estonia. In this comparison, we found a very good correlation, although it is emphasized that this four-week study period is rather short to be compared against previous MODIS validation studies with longer-term data sets. However, our results clearly indicate the potential MODIS AOD data offer in AOD monitoring. During this event of biomass burning aerosols, clear AOD variability was apparent in the measurements. This large range in AOD obviously partly explains the high correlation ($\sim$0.97) between MODIS and AERONET measurements.

The day-to-day AOD variability was also investigated using HYSPLIT generated trajectories. The 24-h backward trajectories were used to assess the origin of the air masses arriving at Tõravere. Together with MODIS Fire Mapper product, they gave further support for those days with low measured AOD (30 April most distinctly) during the episode of otherwise elevated aerosol loading.

In the second part of our paper, we discussed the impact that this intrusion of biomass burning aerosols had on the surface radiation levels measured in southern Finland. The station of Jokioinen is not generally influenced by industrial or urban activities to any large extent. Therefore, it was an ideal site to study the radiative effects exerted by the transport of biomass burning aerosols. For this purpose, we used both UV and global irradiance at Jokioinen. Many days with cloudless weather made possible a more detailed analysis of how this episode reduced the surface irradiances. The study period exhibited a rather strong short-term variability in the surface irradiances (for instance, around 29 April to 1 May). The good agreement between polluted model run and measurements suggests that the MODIS AOD used for UV wavelengths in our radiative transfer calculations is representative for the real conditions, and also well captures the day-to-day AOD variability. Reductions of up to 35% compared to typical aerosol conditions were found at 340 nm. For global radiation, the reduction was always smaller, in line with the expected wavelength dependence of the aerosol effect. Our results are comparable to the aerosol-induced UV reduction given, for instance, by Kalashnikova et al. (2007) for biomass burning aerosols in Australia. They reported 20–25% decrease in UV at 320–400 nm, for an aerosol loading similar to the average during event studied in this paper (with AOD of 0.6 at 500 nm).

Acknowledgements. The authors gratefully acknowledge the NOAA Air Resources Laboratory (ARL) for the provision of the READY website (http://www.arl.noaa.gov/ready.html) used in this publication. The authors would also like to acknowledge the MODIS Teams for their effort in making the aerosol data available. We also thank O. Kärner, and his team at Tõravere, for establishing and maintaining AERONET Tõravere site. One of the authors (AL) wishes to acknowledge the support from the SCOUT-O3 project (505390-574 GOCE-CT-2004).

Edited by: A. Petzold

References

Anderson, G. P., Clough, S. A., Keizys, F. X., Chetwynd, J. H., and Shettle, E. P.: AFGL atmospheric constituent profiles (0–120 km), Environmental Research Papers, United States. Air Force Geophysics Lab., Hanscom AFB, MA,954, 1–43, 1986.

Balis, D. S., Amiridis, V., Zerefos, C., Kazantzidis, A., Kazadzis, S., Bais, A. F., Meleti, C., Gerasopoulos, E., Papayannis, A., Matthias, V., Dier, H., and Andreae, M. O.: Study of the effect of different type of aerosols on UV-B radiation from measurements during EARLINET, Atmos. Chem. Phys., 4, 307–32, 2004, http://www.atmos-chem-phys.net/4/307/2004/.

Christopher S. A. and Zhang, J. L.: Cloud-free shortwave aerosol radiative effect over oceans: Strategies for identifying anthropogenic forcing from Terra satellite measurements, Geophys. Res. Lett., 31, L18101, doi:10.10292004GL020510, 2004.

Chu, D. A., Kaufman, Y. J., Ichoku, C., Remer, L. A., Tanre, D., and Holben, B.: Validation of MODIS aerosol optical depth retrieval over land, Geophys. Res. Lett., 29, 8007, doi:10.1029/2001GL013205, 2002.

Erlick, C. and Frederick, J. E.: Effects of aerosols on the wavelength dependence of atmospheric transmission in the ultraviolet and visible 2. Continental and urban aerosols in clear skies, J. Geophys. Res., 103(D18), 23 275–23 286, 1998.

Holben, B. N., Eck, T. F., Slutsker, I., Tanre, D., Buis, J. P., Setzer, A., Vermote, E., Reagan, J. A., Kaufman, Y., Nakajima, T., Lavenu, F., Jankowiak, I., and Smirnov, A.: AERONET – A federated instrument network and data archive for aerosol characterization, Rem. Sens. Environ., 66(1), 1–16, 1998.

Kalashnikova, O. V., Franklin, P. M., Eldering, A., and Anderson, D.: Application of satellite and ground-based data to investigate the UV radiative effects of Australian aerosols Rem. Sens. Environ., 107, 65–80, 2007.

Kato, S., Ackerman, T. P., Mather, J. H., and Clothiaux, E. E.: The k-distribution method and correlated-k approximation for a shortwave radiative transfer model, J. Quant. Spectrosc. Radiat. Transfer, 62, 109–121, 1999.

Koepke, P., M., Schult, I., and Shettle, E. P.: Global Aerosol Data Set, Max-Planck-Institut für Meteorologie, 243, Hamburg, Germany, 1997.

Koskela T. (Ed.): The Nordic Intercomparison of ultraviolet and total ozone instruments at Izaa from 24 October to 5 November 1993, final rep., 27 Finnish Meteorol. Inst., Helsinki, 1994.

Krotkov, N. A., Bhartia, P. K., Herman, J. R., Fioletov, V., and Kerr, J.: Satellite estimation of spectral surface UV irradiance in the presence of tropospheric aerosols 1. Cloud-free case, J. Geophys. Res., 103(D8), 8779–8794, 1998.

Kylling, A., Bais, A. F., Blumthaler, M., Schreder, J., Zerefos, C. S., and Kosmidis, E.: Effect of aerosols on solar UV irradiances during the Photochemical Activity and Solar Ultraviolet Radiation campaign, J. Geophys. Res., 103(D20), 26 051–26 060, 1998.

Lindfors, A., Arola, A., Kaurola, J., Taalas, P., and Svenøe, T.: Long-term erythemal UV doses at Sodankylä estimated using total ozone, sunshine duration, and snow depth, J. Geophys. Res., 108(D16), 4518, doi:10.1029/2002JD003325, 2003.

Madhavi Latha, K., Badarinath, K. V. S., Gupta, P. K., et al.: Impact of biomass burning aerosols on UV erythema – a case study from northeast region of India, J. Atmos. Solar-Terr. Phys., 66, doi:10.1016/j.Jastp.2004.03.005, 2004.

Mayer, B. and Kylling, A.: Technical note: The libRadtran software package for radiative transfer calculations – description and examples of use, Atmos. Chem. Phys., 5, 1855–1877, 2005, http://www.atmos-chem-phys.net/5/1855/2005/.

Remer, L. A., Tanré, D., Kaufman, Y. J., et al.: Validation of MODIS aerosol retrieval over ocean, Geophys. Res. Lett., 29, 8008, doi:10.1029/2001GL013204, 2002.

Remer, L. A., Kaufman, Y. J., Tanré, D., et al.: The MODIS Aerosol Algorithm, Products, and Validation, J. Atmos. Sci., 62, 947–973, 2005.

Reuder J. and Schwander, H.: Aerosol effects on UV radiation in non-urban regions, J. Geophys. Res., 104, 4065–4067, 1999.

Rolph, G. D.: Real-time Environmental Applications and Display sYstem (READY) Website (http://www.arl.noaa.gov/ready/hysplit4.html). NOAA Air Resources Laboratory, Silver Spring, MD, 2003.

Seckmeyer, G., Bais, A., Bernhard, G., Blumthaler, M., Booth, C. R., Disterhoft, P., Erikson, P., McKenzie, R. L., Miyauchi, M., and Roy, C.: Instruments to measure solar ultraviolet radiation, Part 1: Spectral instruments, World Meteorological Report 125, WMO TD 1066, 2001.

Shettle, E. P.: Models of aerosols, clouds and precipitation for atmospheric propagation studies, Atmospheric Propagation in the UV, Visible, IR and mm-region and Related System Aspects, AGARD Conf. Proc., 454, 15-1–15-13, 1989.

Stohl, A., Berg, T., Burkhart, J. F., Fjæraa, A. M., Forster, C., Herber, A., Hov, Ø., Lunder, C., McMillan, W. W., Oltmans, S., Shiobara, M., Simpson, D., Solberg, S., Stebel, K., Ström, J., Tørseth, K., Treffeisen, R., Virkkunen, K., Yttri, K. E.: Arctic smoke record high air pollution levels in the European Arctic due to agricultural fires in Eastern Europe, Atmos. Chem. Phys., 7, 511–534, 2007, http://www.atmos-chem-phys.net/7/511/2007/.

Uppala, S., Kållberg, P., Simmons, A., Andrae, U., da Costa Bechtold, V., Fiorino, M., Gibson, J., Haseler, J., Hernandez, A., Kelly, G., Li, X., Onogi, K., Saarinen, S., N. Sokka, R. Allan, E. Andersson, K. Arpe, M. Balmaseda, Beljaars, A., van de Berg, L., Bidlot, J., Bormann, N., Caires, S. Chevallier,, F., Dethof, A., Dragosavac, M., Fisher, M., Fuentes, M., Hagemann, S., Holm, E., Hoskins, B., Isaksen, L., Janssen, P., Jenne, R., McNally, A., Mahfouf, J.-F., Morcrette, J.-J., Rayner, N., Saunders, R., Simon, P., Sterl, A., Trenberth, K., Untch, A., Vasiljevic, D., Viterbo, P., and Woollen, J. : The ERA-40 re-analysis, Q. J. R. Meteorol. Soc., 131, 2961–3012, doi:10.1256/qj.04.176, 2005.

Yu, H., R. E.,, M. Chin, Kaufman, Y. J., Zhou, M., Zhou, L., Tian, Y., Dubovik, O., and Holben, B. N.: Direct radiative effect of aerosols as determined from a combination of MODIS retrievals and GOCART simulations, J. Geophys. Res., 109, D03206, doi:10.1029/2003JD003914, 2004.